

Effect of Wall Shear Stress on Myoblast Orientation Distribution

Hiroki YONEZAWA

Biomedical Engineering, Systems Design, Kogakuin University
Tokyo, 163-8677, Japan

Shigehiro HASHIMOTO

Biomedical Engineering, Department of Mechanical Engineering, Kogakuin University
at13351@g.kogakuin.jp Tokyo, 163-8677, Japan

Ryuya ONO

Biomedical Engineering, Mechanical Engineering, Kogakuin University
Tokyo, 1638677, Japan

ABSTRACT

The effect of wall shear stress on the orientation of cells was examined *in vitro*. Couette-type shear flow device was made between the lower fixed culture plate and the upper rotating disk with a fixed gap. After 24 hours of no-flow culture to allow cell attachment to the lower culture disc, shear stress of 2 Pa or less was continuously applied to the mouse myoblasts (C2C12) for 24 hours in the incubator. The behavior (deformation and major axis angle) of each cell was tracked by time-lapse images observed with an inverted phase contrast microscope placed in the incubator. At a shear stress of around 1 Pa, cells tend to orient parallel to the shear stress direction. Around 1.4 Pa, several cells tend to deviate from the shear stress direction. Around 1.8 Pa, the cell is widely distributed at various angles. Cells tend to grow longer in the higher shear stress field in all directions, regardless of the direction of shear stress below 2 Pa. The experimental results would be applied to control the orientation of cells in the engineered tissue.

Keywords: Biomedical Engineering, Cell Culture, Shear Stress, Deformation, Orientation, C2C12 and Couette Flow.

1. INTRODUCTION

Biological cells migrate on scaffolds. Cells are exposed to shear stress both *in vivo* and *in vitro*. The direction of the shear stress field can affect the direction of cell deformation [1]. Under wall shear stress, cells exhibit responses such as elongation, tilting to the streamline, migration [2], deformation [3], division [4], differentiation [5] and detachment from the scaffold wall.

In the Hagen-Poiseuille flow, the shear rate depends on the distance from the wall and is highest at the wall. In a Couette type flow, on the other hand, the shear rate is constant regardless of the distance from the wall [6].

The effects of shear flow on endothelial cells exposed to blood flow on the inner surface of the vessel wall have been examined in many studies [7, 8]. In the previous study with the vortex flow [9], endothelial cells oriented along the streamlines, whereas myoblasts oriented perpendicular to the streamlines [10]. The orientation of each cell in a tissue depends on the orientation of neighboring cells [11, 12].

In this study, the effect of wall shear stress on myoblast orientation distribution [13] has been tracked by time-lapse microscopy images observed using the Couette-type flow device placed in an incubator.

2. MATERIALS AND METHODS

Shear Flow Device for Cell Culture

To apply the constant shear flow field to the cell culture, a Couette type of shear flow device has been used (Fig. 1). The shear field is generated between a rotating disk and a stationary dish. The medium is sheared between a rotating wall and a stationary wall. The stationary wall is the bottom of the culture dish (diameter 60 mm).

In the device, the shear rate (γ) in the medium is calculated by Eq. (1).

$$\gamma = r \omega / d \quad (1)$$

In Eq. (1), ω is the angular velocity, and d is the gap between the wall of the moving disk and the wall of stationary plate. Between the parallel walls, d is constant. The shear rate (γ) in the gap between walls increases in proportion to the distance (r) from the axis of the rotation.

The angular velocity ω (< 22 rad/s) was controlled by the stepping motor. In the observation area of the microscope, r varies between 17 mm and 18 mm. The distance d , which was measured by the positions of the focus of the walls at the microscope, was around 0.6 mm. The shear rates (γ) of 6.7×10^2 s⁻¹ are made in the present experiment by adjustment of these parameters.

The shear stress (τ) is calculated by the viscosity (η) of the medium.

$$\tau = \eta \gamma \quad (2)$$

Using the viscosity of the medium of 1.5×10^{-3} Pa s (measured by a cone and plate viscometer at 310 K), the shear stress τ have been calculated as the value of 1 Pa.

The rotating disk device is mounted on the stage of the inverted phase contrast microscope placed in the incubator. The device

allows the microscopic observation of cells cultured on the stationary wall during exposure to the shear flow field.

Cultured Cell

C2C12 (mouse myoblast cell line originated with cross-striated muscle of C3H mouse, passage between eight and ten) were used in the test. Cells were cultured in D-MEM (Dulbecco’s Modified Eagle’s Medium): containing 10% decomplexed FBS (fetal bovine serum), and 1% penicillin/ streptomycin.

The cells were seeded on the dish at the density of 3000 cells/cm². To make adhesion of cells to the bottom of the culture dish, the cells were cultured for 24 hours in the incubator without flow stimulation (without rotation of the disk).

After the pre-incubation for 24 hours without shear, the cells were continuously sheared with the rotating disk for 24 hours in the incubator at the constant rotating speed. The constant speed was preset for each test to keep the designed shear stress field.

Analysis of Cell Behavior

The time-lapse microscopic image was taken every ten minutes during the cultivation. The contour of each cell adhered on the stationary plate of the scaffold was traced (Fig. 2). The contour of each cell was approximated to ellipse in two-dimensional image.

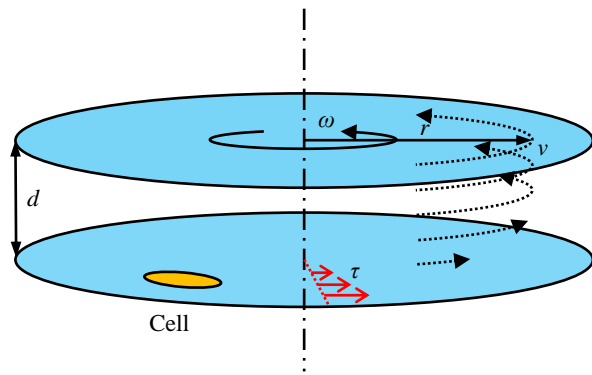


Fig. 1: Couette flow (velocity (v) distribution) between rotating (angular velocity ω) wall and stationary wall at r (radius) (distance d): wall shear stress (τ).

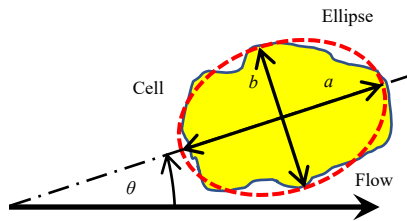


Fig. 2: Shape index and angle (θ) of cell exposure to flow.

On the ellipse, the length of the major axis (a), and the length of the minor axis (b) were measured. The ratio of axes is calculated as the shape index (P) by Eq. (3).

$$P = 1 - b / a \tag{3}$$

At the circle, $P = 0$. As the ellipse is elongated, P approaches to one. The acute angle (θ) between the major axis and the flow direction was measured counterclockwise (Fig. 2).

3.RESULTS

Figs. 3-5 shows the cumulative data for 24 hours, where n_0 is the initial number of cells. Each point corresponds to the data of each cell at each instant in the time-lapse images.

Fig. 3 shows the direction angle (θ) of the long axis of each cell in relation to the shear stress (τ). Under the shear flow for 24 hours, the cells make rotation, deformation, and division. Figs. 3a-3c, Figs. 4a-4c and Figs. 5a-5c show data of sparsely distributed cells. Cells made several colonies in Fig. 3d, Fig. 4d, and Fig.5d. Cells were confluent in Fig. 3e, Fig. 4e, and Fig.5e.

At a shear stress of around 1 Pa, many of the angle data are distributed around 0 degrees (Figs. 3a, 3e). Around 1.4 Pa, the shear stress is mostly distributed in the negative direction (Fig. 3b). Around 1.8 Pa, the cell is widely distributed at various angles (Fig. 3c). When cells are in colonies or in confluent layers, they are widely distributed at various angles at a shear stress of around 1 Pa (Figs. 3d, 3e).

Around 1 Pa, many of the shape indexes are distributed around 0.6 (Fig. 4a). At around 1.4 Pa and 1.8 Pa, many of the shape indexes are distributed around 0.8 (Figs. 4b, 4c). When cells are in colonies or in confluent layers, many of the shape indexes are distributed above 0.6 (Figs. 4d, 4e). Around 1.4 Pa, many of the shape indexes are distributed around 0.8 at the negative angles (Fig. 5b).

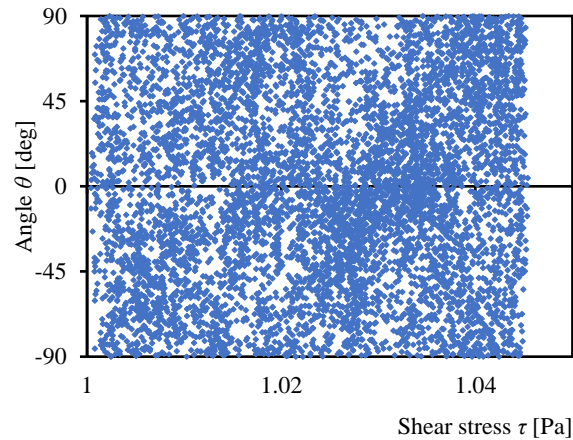


Fig. 3a: Angle θ vs. shear stress τ ($1 \text{ Pa} < \tau < 1.05 \text{ Pa}$); $n_0 = 137$.

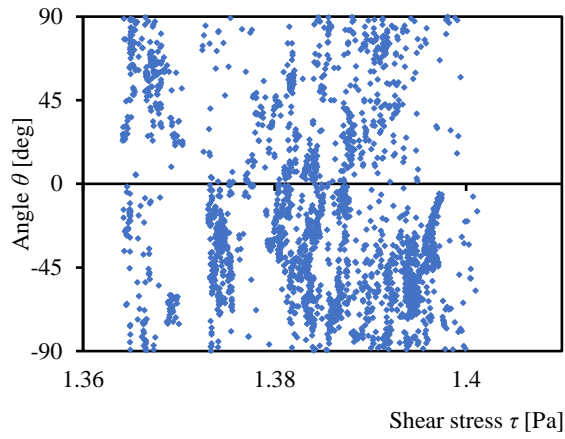


Fig. 3b: Angle θ vs. shear stress τ ($1.36 \text{ Pa} < \tau < 1.41 \text{ Pa}$); $n_0 = 17$.

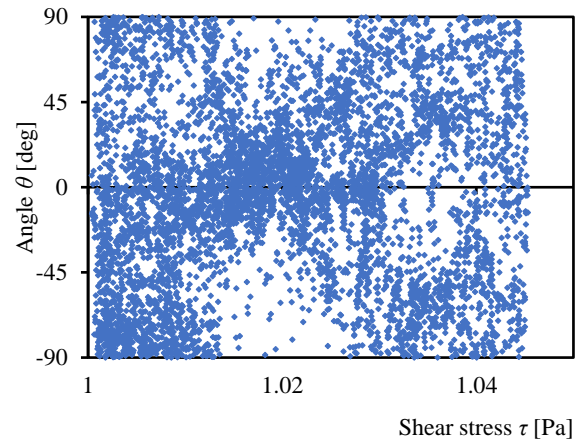


Fig. 3e: Angle θ vs. shear stress τ ($1.00 \text{ Pa} < \tau < 1.05 \text{ Pa}$); $n_0 = 404$.

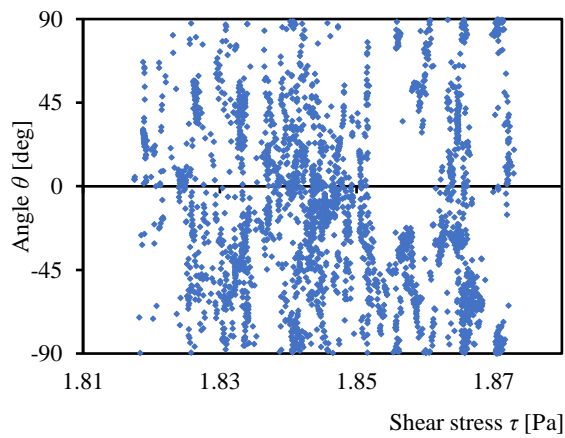


Fig. 3c: Angle θ vs. shear stress τ ($1.81 \text{ Pa} < \tau < 1.88 \text{ Pa}$); $n_0 = 43$.

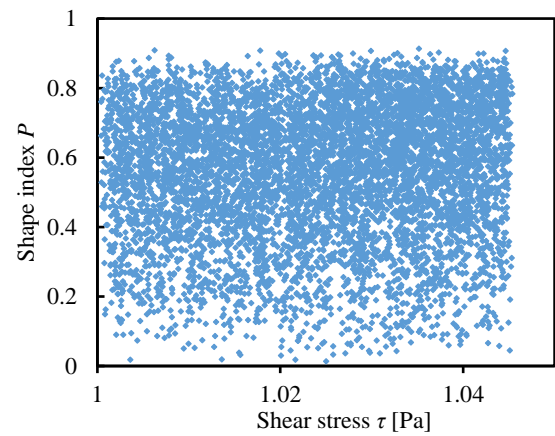


Fig. 4a: Shape index P vs. shear stress τ ($1.00 \text{ Pa} < \tau < 1.05 \text{ Pa}$); $n_0 = 137$.

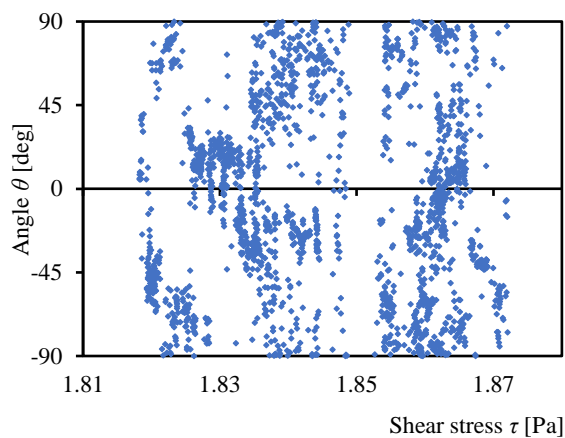


Fig. 3d: Angle θ vs. shear stress τ ($1.81 \text{ Pa} < \tau < 1.88 \text{ Pa}$); $n_0 = 218$.

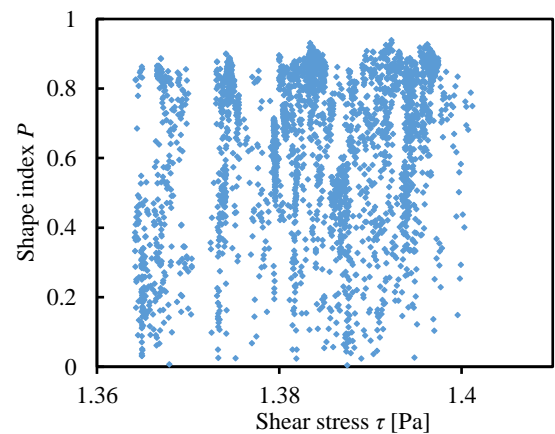


Fig. 4b: Shape index P vs. shear stress τ ($1.36 \text{ Pa} < \tau < 1.41 \text{ Pa}$); $n_0 = 17$.

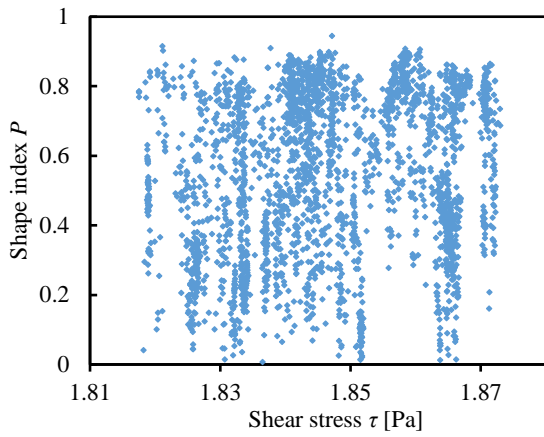


Fig. 4c: Shape index P vs. shear stress τ ($1.81 \text{ Pa} < \tau < 1.88 \text{ Pa}$); $n_0 = 43$.

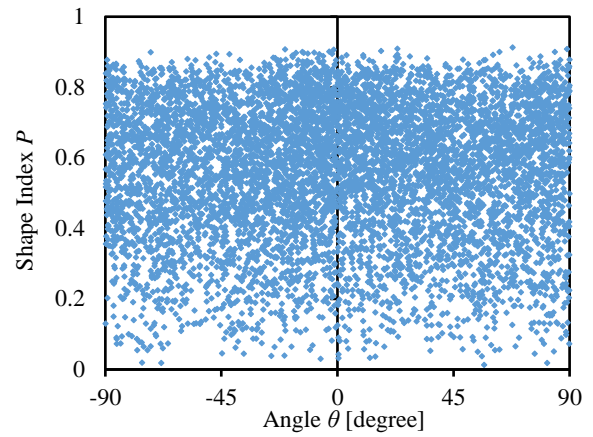


Fig. 5a: Shape index P vs. angle θ ; shear stress τ ($1.00 \text{ Pa} < \tau < 1.05 \text{ Pa}$); $n_0 = 137$.

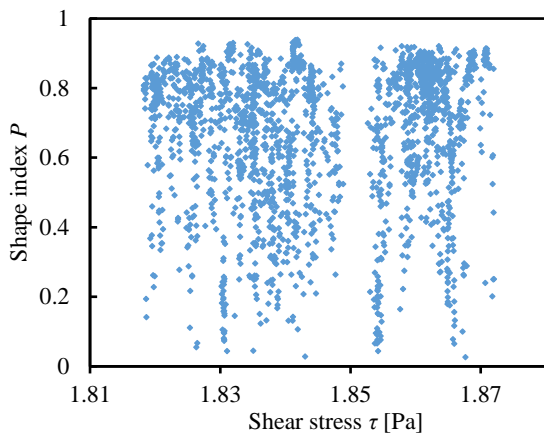


Fig. 4d: Shape index P vs. shear stress τ ($1.81 \text{ Pa} < \tau < 1.88 \text{ Pa}$); $n_0 = 218$.

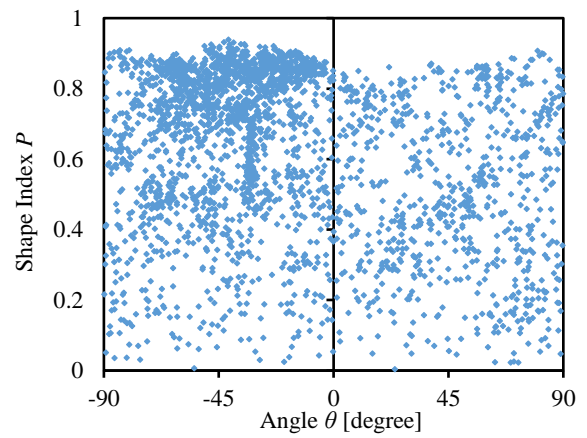


Fig. 5b: Shape index P vs. angle θ ; shear stress τ ($1.36 \text{ Pa} < \tau < 1.41 \text{ Pa}$); $n_0 = 17$.

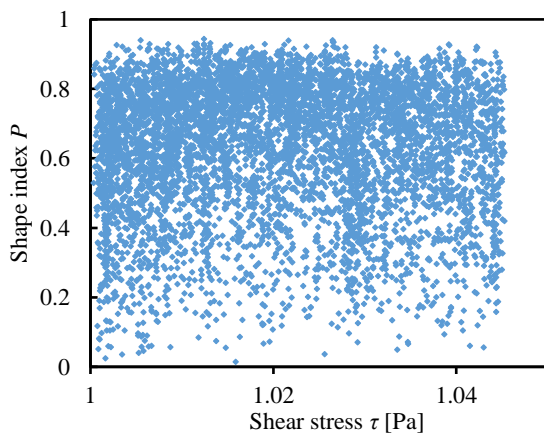


Fig. 4e: Shape index P vs. shear stress τ ($1.00 \text{ Pa} < \tau < 1.05 \text{ Pa}$); $n_0 = 404$.

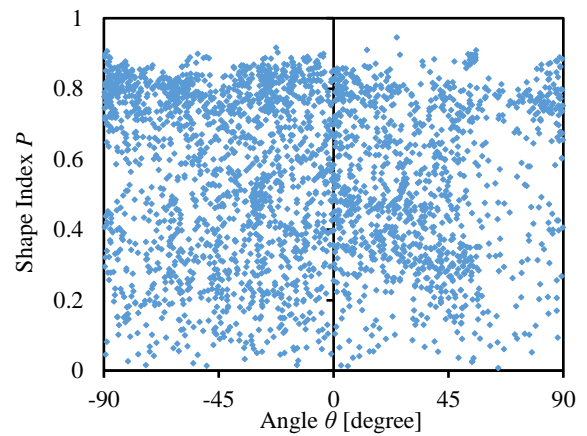


Fig. 5c: Shape index P vs. angle θ ; shear stress τ ($1.81 \text{ Pa} < \tau < 1.88 \text{ Pa}$); $n_0 = 43$.

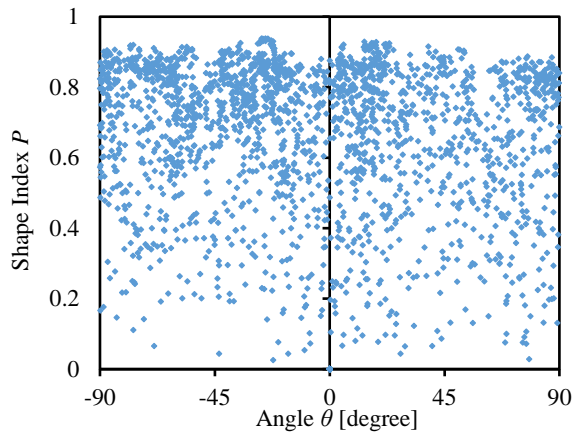


Fig. 5d: Shape index P vs. angle θ ; shear stress τ ($1.81 \text{ Pa} < \tau < 1.88 \text{ Pa}$); $n_0 = 218$.

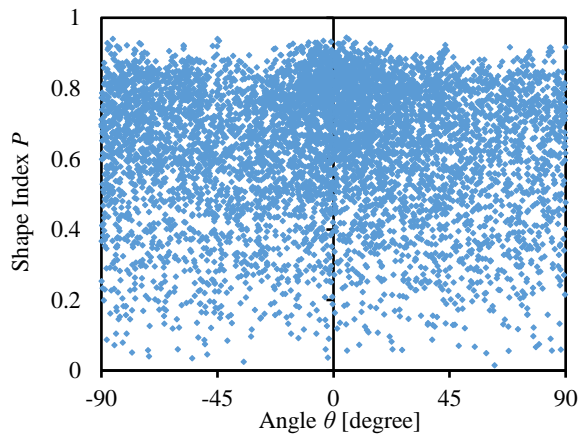


Fig. 5e: Shape index P vs. angle θ ; shear stress τ ($1.00 \text{ Pa} < \tau < 1.05 \text{ Pa}$); $n_0 = 404$.

4. DISCUSSION

In this study, the orientation and shape of C2C12 in a shear flow field were observed at time-lapse images. A Couette-Flow device that generates the shear flow in the culture medium in a culture dish was used. The relationship between the shear stress and the response of C2C12 was analyzed. The shear stress below 2.0 Pa is typical value for the wall shear stress at the blood vessels *in vivo*. Because the cell division [4] was not the main topic in this study, the observation time was limited within 24 hours.

The wall shear stress gradient along the radial direction [14] was less than 0.1 Pa/mm in this study. The difference of the shear stress was less than 0.01 Pa between locations with a distance of 0.1 mm. The elongated cells are less than 0.1 mm in length. At the shear stress field higher than 1 Pa, cells tended to move from the position with the negative angle. In previous studies, C2C12 tended to migrate to the direction of low shear stress [15] in sparsely distributed cells.

The wall shear stress of 1 Pa is a typical value for the inner surface of human blood vessels *in vivo*. Endothelial cells are exposed to shear stress of about 1 Pa, and most myoblasts tend to migrate obliquely downward in the shear stress field of 1 Pa. The effect of shear flow on cells depends on the cell type [16]. This dependence may be applicable to cell sorting technology. To study the initial behavior of cells, it is convenient to follow the cells after they have divided [4]. Cells proliferate regardless of shear flow stimulation. The cell cycle did not change regardless of shear flow stimulation. In the present experiment, it was possible to follow the deformation of each cell by time-lapse images taken at 10-minute intervals.

Many studies have been conducted on the effects of shear flow on cells. Shear flow affects the adhesion of each cell. Cell adhesion can be controlled by the design of scaffolds [17]. Simulation of cell behavior in shear flow shows that shear flow affects cell adhesion. The effect of fluid-induced shear stress on osteoblasts was investigated [5]. The behavior of endothelial cells can be a sensor of fluid shear stress [7]. The force field parallel to the scaffold surface also can affect cell behavior [18].

The effects of shear stress gradients on cells have also been investigated [8]. Wall shear stress gradients can cause elongated cells to rotate counterclockwise [3, 14]. It was shown that endothelial cells tend to tilt in a direction parallel to the flow direction when the wall shear stress is 1.8 Pa or higher. At shear stresses above 0.5 Pa, the endothelial cells tended to elongate.

The cells change into spheres when they divide. A sphere is a circle on a two-dimensional projection plane. The shape index (P) of the circle is zero. When the cells are highly active, the data of shape index (P) are widely distributed under the wall shear stress stimulus ($0.5 \text{ Pa} < \tau < 2 \text{ Pa}$) for each cell. Moderate wall shear stress promotes active deformation of each cell. Excessive wall shear stress may induce detachment of cells from the culture surface scaffold. Regardless of the cell type, the number of detached cells increases as the shear stress approaches 2.0 Pa.

The behavior of each cell depends on its neighbors [11, 12]. Since the initial number of cells in the image corresponding to each figure is not controlled to be constant, it is not possible to compare the absolute number of cells beyond the figure number. Since the data in each figure were collected from the same time-lapse images in the same observation area of the experiment, the relative distributions are comparable. The experimental results would be applied to control the orientation of cells in the engineered tissue.

5. CONCLUSION

Myoblasts were cultured under wall shear stress between 1 Pa and 2 Pa *in vitro*. A Couette flow experimental system with a rotating disk in a parallel position with a fixed gap was designed to apply shear stress to cells. Time-lapse images were analyzed using ImageJ to trace the shape and orientation of the cells. At a shear stress of around 1 Pa, cells tend to orient parallel to the shear stress direction. Around 1.4 Pa, several cells tend to deviate from the shear stress direction. Around 1.8 Pa, the cell is widely distributed at various angles. Cells tend to grow longer in the higher shear stress field in all directions, regardless of the direction of shear stress below 2 Pa.

ACKNOWLEDGMENT

The authors thank Mr. Hiromi Sugimoto for the help of the experiment.

REFERENCES

- [1] J. Ando and K. Yamamoto, "Hemodynamic Forces, Endothelial Mechanotransduction, and Vascular Diseases", **Magnetic Resonance in Medical Sciences**, Vol. 21, No. 2, 2022, pp. 258-266.
- [2] Z. Yan, D. Guo, R. Tao, X. Yu, J. Zhang, Y. He, J. Zhang, J. Li, S. Zhang and W. Guo, "Fluid Shear Stress Induces Cell Migration via RhoA-YAP1-autophagy Pathway in Liver Cancer Stem Cells", **Cell Adhesion and Migration**, 16(1), (2022), pp. 94-106.
- [3] Hashimoto, S., and Yonezawa, H., "Tracings of Behavior of Myoblasts Cultured Under Couette Type of Shear Flow Between Parallel Disks", **Proc. ASME Fluids Engineering Division Summer Meeting (FEDSM2021)**, 2021, pp. 1-7.
- [4] Hashimoto, S., Yonezawa, H., and Ono, R., "Cell Activity Change After Division under Wall Shear Stress Field", **Proc. ASME International Mechanical Engineering Congress & Exposition (IMECE2021)**, 2021, pp. 1-8.
- [5] P.V. Hinton, K.J. Genoud, J.O. Early, F.J. O'Brien and O.D. Kennedy. "Impact of Fluid Flow Shear Stress on Osteoblast Differentiation and Cross-Talk with Articular Chondrocytes", **International Journal of Molecular Sciences**, Vol. 23, No. 16, 2022, pp 1-16.
- [6] S. Hashimoto, H. Sugimoto and H. Hino, "Behavior of Cell in Uniform Shear Flow Field between Rotating Cone and Stationary Plate", **Journal of Systemics Cybernetics and Informatics**, Vol. 16, No. 2, 2018, pp. 1-7.
- [7] E. Roux, P. Bougaran, P. Dufourcq and T. Couffignal, "Fluid Shear Stress Sensing by the Endothelial Layer", **Frontiers in Physiology**, Vol. 11, Article 861, 2020, pp. 1-17.
- [8] K. Kanno, H. Akabane, Y. Shimogonya and N. Kataoka, "Response of Human Endothelial Cells to the Vortex Flow in an Immediately Expanding Flow Chamber", **Journal of Biomechanical Science and Engineering**, Vol. 17, No. 3, 2022, pp. 1-10.
- [9] P. Limraksasin, Y. Kosaka, M. Zhang, N. Horie, T. Kondo, H. Okawa, M. Yamada and H. Egusa, "Shaking Culture Enhances Chondrogenic Differentiation of Mouse Induced Pluripotent Stem Cell Constructs", **Scientific Reports**, Vol. 10, No. 1, 14996, 2020, pp. 1-15.
- [10] S. Hashimoto and M. Okada, "Orientation of Cells Cultured in Vortex Flow with Swinging Plate In Vitro", **Journal of Systemics Cybernetics and Informatics**, Vol. 9, No. 3, 2011, pp. 1-7.
- [11] S. Hashimoto and T. Yokomizo, "Tracings of Interaction Between Myoblasts Under Shear Flow in Vitro", **Proc. ASME Fluids Engineering Division Summer Meeting (FEDSM2021)**, 2021, pp. 1-9.
- [12] S. Hashimoto, T. Yokomizo and Y. Endo, "Behavior of Myoblasts in Two-dimensional Colony under Shear Flow Field", **Proc. 13th International Multi-Conference on Complexity Informatics and Cybernetics**, Vol. 2, 2022, pp. 7-11.
- [13] H. Yonezawa, S. Hashimoto, H. Kinoshiro and Yuta Nagasawa, "Effect of Wall Shear Stress on Endothelial Cells Orientation Distribution", **Proceedings of the 26th World Multi-Conference on Systemics, Cybernetics and Informatics**, 2022, Vol. 2, pp. 44-49.
- [14] H. Yonezawa, S. Hashimoto and R. Ono, "Effect of Wall Shear Stress Gradient on Cell: Distribution of Deformation and Rotation", **Proc. 13th International Multi-Conference on Complexity Informatics and Cybernetics**, Vol. 2, 2022, pp. 53-58.
- [15] S. Hashimoto, H. Sugimoto and H. Hino, "Effect of Couette Type of Shear Stress Field with Axial Shear Slope on Deformation and Migration of Cell: Comparison between C2C12 and HUVEC", **Journal of Systemics Cybernetics and Informatics**, Vol. 17, No. 2, 2019, pp. 4-10.
- [16] S. Hashimoto, K. Yoshinaka and H. Yonezawa, "Behavior of Cell Under Wall Shear Stress in Flow Field: Comparison Among Cell Types", **Proc. ASME Fluids Engineering Division Summer Meeting (FEDSM2021)**, 2021, pp. 1-8.
- [17] M. Xu, T. Su, X. Jin, Y. Li, Y. Yao, K. Liu, K. Chen, F. Lu and Y. He, "Inflammation-mediated Matrix Remodeling of Extracellular Matrix-mimicking Biomaterials in Tissue Engineering and Regenerative Medicine", **Acta Biomaterialia**, Vol. 151, 2022, pp. 106-117.
- [18] S. Hashimoto, "Effect of Force Field on Deformation and Migration of Single Cell with Orientation Controlled by Micro-Striped Topography Patterns", **ASME Journal of Engineering and Science in Medical Diagnostics and Therapy**, Vol. 6, 2023, pp. 1-6 (JESMDT-22-1054).